**Optical Tweezers**

**Using the Texas Instruments'**

**Digital Micromirror Device™**

by

Jeremy R. Hui

Submitted to the Department of Electrical Engineering and Computer Science

in Partial Fulfillment of the Requirements for the Degrees of

Bachelor of Science in Electrical Science and Engineering

and Master of Engineering in Electrical Engineering and Computer Science

at the Massachusetts Institute ofTechnology

May 23, 2001







Author_____
Department of Electrical Engineering and Computer Science
May 23, 2001

Certified by_____ 5/18/01
Richard Gale
VI-A Company Thesis Supervisor

Certified by_____ 5/23/01
Rajeev Ram
M.I.T. Thesis Supervisor

Accepted by_____
Arthur C. Smith
Chairman, Department Committee on Graduate Theses

Optical Tweezers
Using the Texas Instruments'
Digital Micromirror Device™
by
Jeremy R. Hui

Submitted to the
Department of Electrical Engineering and Computer Science
May 23, 2001

In Partial Fulfillment of the Requirements for the Degrees of
Bachelor of Science in Electrical Science and Engineering
and Master of Engineering in Electrical Engineering and Computer Science
at the Massachusetts Institute ofTechnology

# ABSTRACT

The Digital Micromirror Device (DMD™) provides an effective method of spatially shuttering monochromatic light as demonstrated with an optical tweezer system. Optical tweezers use laser light to trap and hold microscopic objects such as biological cells. Integrating the DMD into the system allows for control over the intensity and location of light in the optical trap. Code for specialized DMD control board was developed to enable computer control over the DMD. Combined with a video framegrabber and image processing code, a feedback system was developed with the goal of automated optical trapping with idenfication and sorting abilities. The system was able to see, identify, and trap 3$\mu$m polystyrene beads using the DMD, but was unable to effectively move the beads to sort them.

VI-A Thesis Supervisor: Dr. Richard Gale, Ph.D.
Title: Distinguished Member, Technical Staff, DLP™ Products Technology Development

Thesis Supervisor: Rajeev Ram
Title: Associate Professor, Electrical Engineering and Computer Science Department

CHAPTER 1

# Optical Tweezer Theory and Operation

Optical tweezers are based on the theory of radiation pressure. By using the various effects of light, dielectric particles ranging in size from submicron to hundreds of microns can be successfully held by a beam (or beams) of light. Initially developed by Ashkin[1] at Bell Labs, optical tweezers are primarily used for trapping biological cells. A variant of the system has also been used to slow and trap individual atoms.

Radiation pressure can be broken into several subforces, two of which are scattering and gradient forces. The scattering force is in the direction of the light away from the source while the gradient force is along the intensity gradient towards the most intense region. The strength of the scattering force is proportional to the light intensity whereas the gradient force is pro-

portional to the gradient of the light intensity. Balancing these forces can create three-dimensionally stable traps.

In the Rayleigh regime where the wavelength of light is much less than the diameter of the object, the trapped objects are modeled as dipole scatterers, simplifying the forces to the electromagnetic field representation of light. The scattering force is proportional to the power scattered and the index of the immersion medium. The gradient force comes from the polarization

$$F_{scat} = n_1 \frac{\langle S \rangle \sigma}{c} \qquad \text{Eq. 1.1}$$

force.[2] It is related to the polarizability of the particle and the gradient of the intensity. The result is a force in the direction of

$$F_{grad} = \frac{\alpha_2}{2} \Delta \langle E^2 \rangle \qquad \text{Eq. 1.2}$$

the gradient of the light.

When applied to particles in the Mie size regime, the forces can be approximated from a ray-optics approach. (Mie implies the diameter is large compared to the wavelength of the light.($\lambda \gg d$)) An incident ray is refracted as it passes through the object; the change of momentum of the light ray equates

into a force. Reflection of the ray mostly causes the scattering

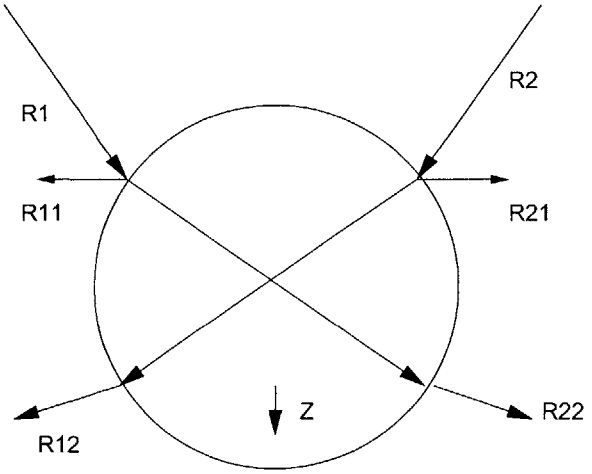


Fig. 1.1: Forces on Sphere Above Light Focal Point

force, while refraction causes the gradient force. With a focused beam of light with a Gaussian intensity profile, the net force is towards the center of the beam and towards the diffraction-limited focus point of the light.

More oblique or peripheral rays create greater forces towards the focus point while direct rays will push the object downstream. (Downstream is defined as away from the light source. Upstream would be towards the light source.) The balance of these rays creates an axially stiff trap. Transverse stiffness is affected by the intensity profile. The steeper the gradient along the beam center line, the stronger the transverse stiffness. This gradient can be naturally created by the Gaussian intensity profile of a laser. As a result, the transverse stiffness is approx-

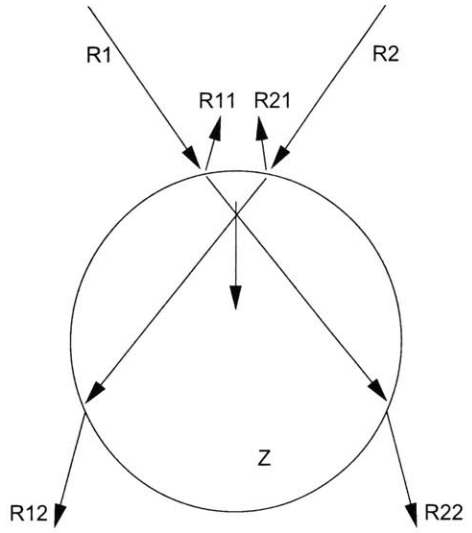


Fig. 1.2: Forces on Sphere Below Light Focal Point

imately 30 times larger than the axial stiffness.[7] By increasing the intensity of the oblique rays, the overall trap can be stiffened. (The axial direction is parallel to the light beam, while lateral or transverse directions are perpendicular to the light. As seen through a microscope, changes in the axial dimension would result in a change of focus while lateral is the visual plane.) High NA oil-immersion objective lens are generally

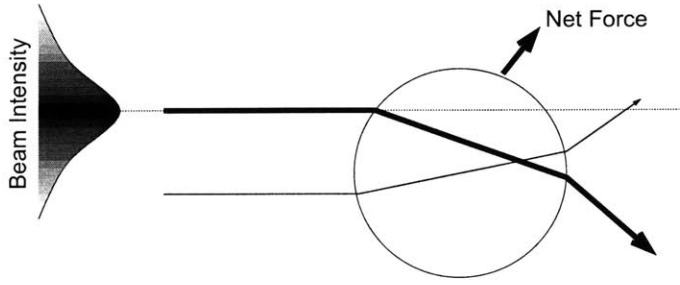


Fig. 1.3

used to create these oblique rays. The use of oil-immersion

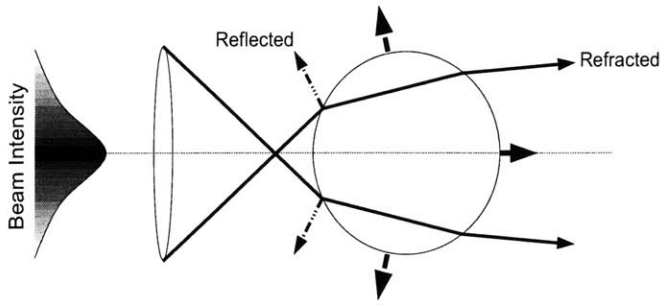


Fig. 1.4

lens, though, causes spherical aberration which causes rays to not come to a single focus. At points near the cover slide surface, this generates greater forces than a comparable water-immersion objective, but comes at the cost of trap stiffness as the trap is moved downwards into the chamber.

The trap strength roughly equal to:

$$F_{trap} = \frac{Qn_1P}{c} \qquad \text{Eq. 1.3}$$

where F is the force acting on the trapped object, Q is a dimensionless efficiency factor, n is the refractive index of the immersion medium, P is the power of the light, and c is the speed of light.[6] Q generally ranges from 0.1 to 0.4 and compensates for the effects of wavelength, spot size, polarization, beam profile, and convergence angle of the laser, and the shape, size,

and refractive index of the trapped object. The resultant forces are generally in the range of piconewtons given milliwatts of input power.

A generalized ray-optics model is generated from the reflection and refraction of an incident light beam.[4] The sum of the rays

$$T_{\backslash\backslash} = \frac{2\sin\theta_t\cos\theta_i}{\sin(\theta_i+\theta_t)\cos(\theta_i-\theta_t)}A_{\backslash\backslash} \qquad \text{Eq. 1.4}$$

$$T_{\perp} = \frac{2\sin\theta_t\cos\theta_i}{\sin(\theta_i+\theta_t)}A_{\perp} \qquad \text{Eq. 1.5}$$

$$R_{\backslash\backslash} = \frac{\tan(\theta_i-\theta_t)}{\tan(\theta_i+\theta_t)}A_{\backslash\backslash} \qquad \text{Eq. 1.6}$$

$$R_{\perp} = \frac{-\sin(\theta_i-\theta_t)}{\cos(\theta_i+\theta_t)}A_{\perp} \qquad \text{Eq. 1.7}$$

*T = transmitted,R = reflected,A = amplitude*
*\\= parallel,⊥= perpindicular*
*$\theta_i$= ∠incident,$\theta_t$= ∠transmitted*

is compared to the incident light to give a resultant force vector for a particular light ray. Then, given a light intensity profile and

an optic system, we sum the force vectors to determine the overall force on the bead and location and stability of any possible optical trap. The rays are assumed to enter the objective plane in a parallel fashion and are focused to a single point. The sphere is assumed to have no absorption. The angle of incidence to a spherical bead is determined from the numerical aperture and the position of the bead.[3] For a stable trap, the sum vector must be zero and for any small displacement, forces must point back to the stable point.

Numerical simulations were performed using this model in a two-dimensional perspective and assuming a circularly polarized beam. The net result is that two stable trapping locations appear to be possible. One trapping location encompasses the focal spot. This would correlate with the highest spot of the intensity and intensity gradient. The second location is further downstream (away from the light source and focal spot.) This location is not as stable, but still appears to have sufficient force to be stable given the proper incident intensity light profile.

Optical traps, as mentioned earlier, are primarily used for biological study. Experiments have been done on bacterial, yeast, and mammalian cells ranging from microsurgery to studying immune response. Additionally, by using polystyrene or silica

beads as micro handles, studies have been done on DNA and protein strengths and structures.[6]

## References

1. A. Ashkin, Dziedzic, J., Optics Letters 11, 288 (1986).
2. N. Simpson, Allen, L., Padgett, M., J. Modern Optics 43, 2485 (1996).
3. S. Smith et al., Am. J. Phys. 67, 26 (1999).
4. M. Born, Wolf, E., *Priniciples of Optics* (Pergamon Press, Oxford, 1970).
5. Z. Hecht, *Optics* (Addison-Wesley, Reading, MA, 1974) p. 40.
6. K. Svoboda, Block, S., Annu. Rev. Biophys. Biomol. Struct. 23, 247 (1994).
7. G. Wuite, Master's Thesis, 1996.

CHAPTER 2

# *Texas Instruments' Digital Micromirror Device™*

The Texas Instruments Digital Micromirror Device™ is the culmination of over 20 years of continuing research and development. Originally designed for printing applications, the DMD™ has since been adapted for other widespread commercial products, the most prominent being projection displays.[1]

The current incarnation of the device consists of a two-dimensional array of tristable mirrors. Each mirror is square and measures 16 $\mu$m across the side. The mirror is rotated about a diagonal into one of three states: 0 degrees, +10 degrees, and -10 degrees. For semantic purposes, the +10 degree state is referred to the on or 1 state, while the -10 degree state is off or 0. The 0 degree position is the parked position. The mirrors are individually controllable by a SRAM cell beneath the mirror

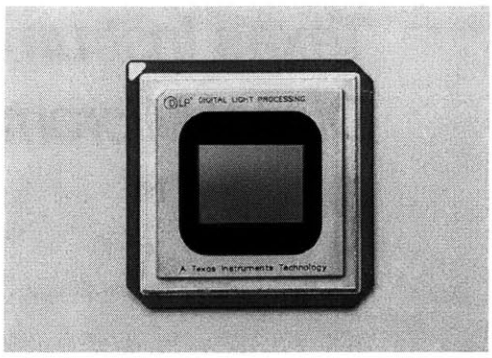


Fig. 2.1: DMD Chip

structure. Writing a 1 into the cell and forcing a global reset pulse will cause the mirror to flip from any state into the +10 degree state. The mirror will hold that position until a new reset pulse is received, regardless of the state of the memory underneath.[2]

The general mirror structure begins with a basic SRAM cell. On top is added the mirror superstructure. The structure has two parts: a lower platform with the drive electrodes and hinge structure and a mushroom-shaped part with the actual mirror surface. Because the hinge lies beneath the actual mirror surface, a 1$\mu$m gap is required between each mirror for proper performance. Additionally, the mirror surface is not completely flat. Due to the processing, the support post has a hole in the center, leaving an approximately 1$\mu$m square gap in the center of the mirror. The mirrors have relatively high performance, with a switching speed around 100$\mu$s.[3,4] The mirrors can

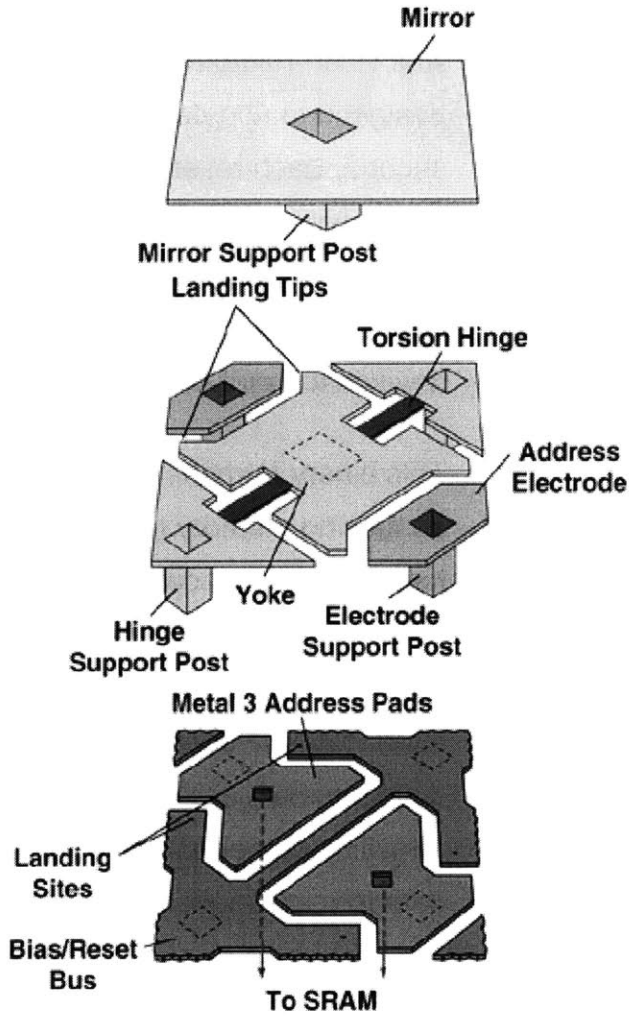


Fig. 2.2: DMD Structure

also hold any given position indefinitely at room temperature without compromising mirror performance[5].

An additional part of this project was the design and construction of a binary formatter. Since the DMD's primary application was video-related applications, the drive electronics were designed to update the mirrors at upwards of 30 frames per second. Each reset pulse causes a momentary flicker in the output light, regardless of the previous or next mirror states. Additionally, the video formatter also is programmed to handle grayscale values. As a result, a binary formatter needed to be devised to reset the mirror states at any arbitrary time.

This binary formatter consists of three main parts: a PCI card containing memory for desired display patterns and control logic, a satellite board with the DMD and actual drive electronics, and software to interface between the user and the PCI card. The software, my main contribution, has two main tasks: interfacing the user commands with the PCI control logic via state registers and a image processing function called a corner turn. The corner turn converts the binary image files into the data format required by the DMD.

The software was broken up into several parts. One section interfaced with the PCI card directly through a software package called WinDriver (Jungo). WinDriver provided the low level hardware access through a C++ code interface (.h files and.lib files). By calling various functions, one can directly read/write

into a section of memory reserved by the PCI card, thus reading/writing into the card resources. It has very little knowledge of the overall system, resulting in little error checking functions. This lack of error checking ability lead to building a dynamic link library (DLL) which encompasses the information about the PCI card, the abilities of the WinDriver code, and the desired user interactions.

Effectively, the DLL provides a higher level access to the PCI card, but it is specific to this particular version of the binary formatter. This allows an end user to write code using the basic DLL functions while we update the binary formatter without forcing the end user to make consequent and required changes to his code. This means that the binary formatter could be upgraded without significant inconvenience, as well as provide extra utility and flexibility for individual end users.

Above the DLL level would exist an end user's code definitions. In this manner, using the functions defined by the binary formatter DLL, the user has wide access to the PCI card resources, but with some error checking built-in. The user can thus create his own application using the binary formatter. Two test applications were a batch file-style interface and a machine vision feedback code for the optical tweezer system. The batch file interface contains several basic commands from

the reading and writing of registers, to the loading and displaying of binary images on the DMD. Its main ability was to read a file of such commands and to execute them, thus the batch file definition. The main purpose of this program is for debugging of the binary formatter card, although it also serves as an initial testbed of the capabilities of the binary formatter. The machine vision feedback code is described in greater depth in Chapter 3. Its main task is to capture video data, analyze it, and return a binary image to the DMD for a feedback system, all working at video frame rates.

Much of the software development process centered around debugging the various interaction issues between the software and hardware. One of the recurring problems was a hanging of all computer processes due to an improper read or write. Most of these were linked to the hardware, particularly how the PCI interface was set up. The hardware side of the binary formatter used a PLX P9050 chip for interacting with the PCI bus, a XILINX FPGA for logic functions, and 128Mb RAM for image storage. The P9050 chip, being designed for a generic application, has many variables, but little error checking. As a result, if certain data registers were set improperly, the PCI bus would not correctly recognize the card or its resources and resulted in a crash of the system. Several weeks were spent debugging the these hardware interactions.

The software package does have several disadvantages. Since the software takes a image file as an input, there is a bit of processing overhead when dealing with file opening. As a result, the DLL had to be customized to compensate for the slow processing time.

### References


1. L. Hornbeck, Texas Inst. Tech. J. 15, 7-46 (1998).
2. M. Mignardi, Texas Inst. Tech. J. 15, 56-63 (1998).
3. R. Meier, Texas Inst. Tech. J. 15, 64-74 (1998).
4. H. Chu et al., Texas Inst. Tech. J. 15, 75-86 (1998).
5. M. Douglass & Sontheimer, A., Texas Inst. Tech. J. 15, 128-136 (1998).

CHAPTER 3

# Optical Tweezer System Design and Layout

The main goal of using the DMD in an optical tweezer setup is to use the computer controlled light modulation ability of the DMD in a fashion that allows for multiple targets to be manipulated and moved in two dimensions.

From the onset, the design of the system assumed that the ray-optic model description was sufficient to describe the stable locations of the trap. Initially, I attempted to design a system that would take the incoming light off each mirror and focus it into a single point. Thus if all the mirrors were on, a plane of diffraction-limited focus points would be generated beneath the objective lens. This idea was discarded for two reasons--the apparent complexity to generate a 1024x768 array of optical elements to individually focus the light from each mirror and

questions regarding how the light forces would behave below the focus plane. With this layout, if multiple mirrors were employed to hold a single object, there didn't seem to be a force-stable point. From the gradient perspective, this layout made sense--a bead would be attracted to the brightest spot in three-dimensional space, or the diffraction limited spot. Using this model, the bead would attempt to encompass as much of the light as possible, with the most stable position being where the gradient was the greatest. By shifting the apparent center of brightness, the bead would attempt to follow the gradient. At the time, though, my understanding of optical design was insufficient to implement such a system.

The other and implemented method of operation revolved around the fact that simulations using the ray-tracing techniques indicated a two stable trapping locations: one at or slightly below the focus point, and one further down below the focus spot, away from the light source. From this assumption, I designed a simple system that spatially shuttered the light entering into a traditional optical tweezer system. The light beneath the objective lens comes to a focus, and based on the mirror states, would form cones extending from the focus. Each cone of light formed by a singular mirror would be combined with other cones to create a larger cone of light strong enough the particle, but only below the focal point. Thus multiple parti-

cles could be held in separate cones of light and transportable by changing the center of the cone in a conveyor belt-like fashion. Controlling the DMD would give the control over the positions of the cones, and therefore, over the trapped particles.

The system construction begins with a basic optical tweezer

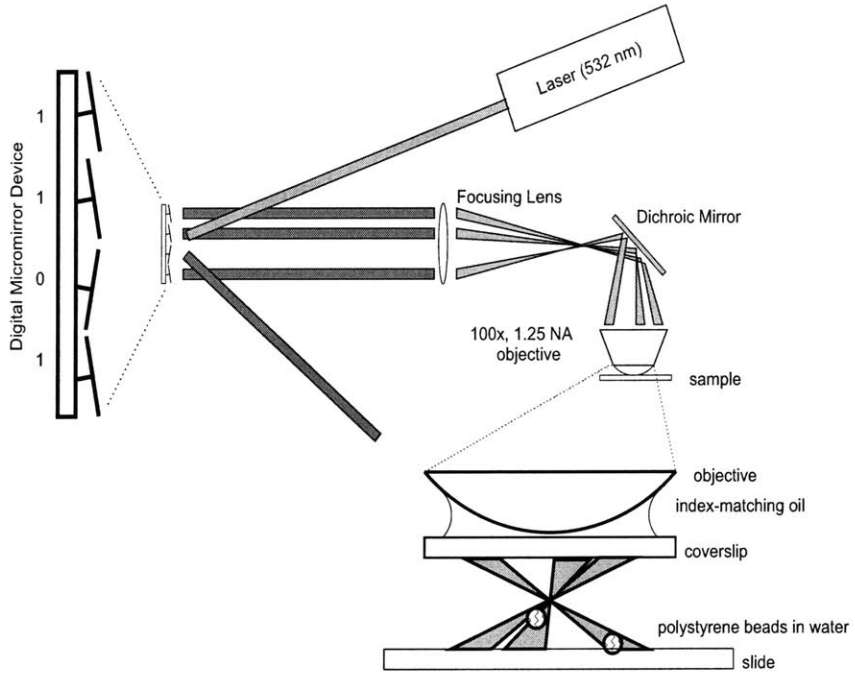


Fig. 3.1: System Diagram

system: a laser passes through an objective lens to the target.[1,2] The target consists of a mixture of water and beads on a glass slide, covered by a coverslip and index matching oil. In this experiment, ordinary tap water was used, although distilled water would have been preferable. The beads used ranged in

size from 0.5$\mu$m to 3.0$\mu$m, with the final data gathered on 3.0$\mu$m beads (Polysciences, Inc). The beads were made of polystyrene, material chosen for the high numerical aperture number(1.6) and a specific gravity density similar to water (1.05). Thus, the beads were expected to float in the liquid for an extended period of time. The coverslip was a #0 thickness (0.13 to 0.17mm). The objective lens was a 100x, 1.25 NA, oil immersion objective with estimated focal length of 0.20mm (Lomo Optics). The laser source was a 532nm, 50mW Nd:YAG, beam diameter of 0.7mm (Coherent Inc.). The laser choice was completely arbitrary as it was the most powerful laser available in the lab at the time. For these experiments,

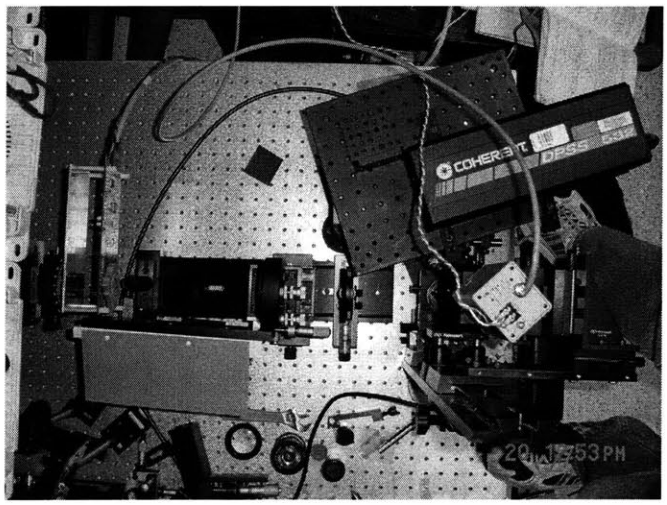


Fig. 3.2: Actual System Viewed From Above

this laser was a decent choice since it was both visible to the naked eye and on the lower end of dangerous in terms of inten-

sity, but still theoretically strong enough to trap beads with only a small portion of the laser energy passing to the end of the system.

To view the beads, a magenta dichroic mirror (Edmund Scientific, Inc.) was employed to redirect the laser beam into the objective lens. This made it possible for a CCD camera to be placed over the objective system and image the beads through the same objective. The CCD was also equipped with a 2x magnifying lens and a polarizing filter to eliminate most of the laser light reflecting towards the camera. The purpose of the 2x TV lens is to increase the imaged size of the beads without seriously affecting the distance of the camera from the objective lens. The polarizing filter eliminates almost all of the stray reflections from the dichroic mirror as well as reflections from the back of the objective. A short tube is also needed to reduce the glare from outside light sources.

Underneath the microscope objective, a simple stage was built using a three-axis lab jack. By having axial control, the stage could perform all focusing functions without affecting the light path of the laser trap. A metal platform with a hole in the center was attached to the jack. The purpose of the hole is to provide some area for illuminating light to pass from the bottom. Initial experiments found that laser light was insufficient to illuminate

the beads for viewing at high objective powers. Thus standard

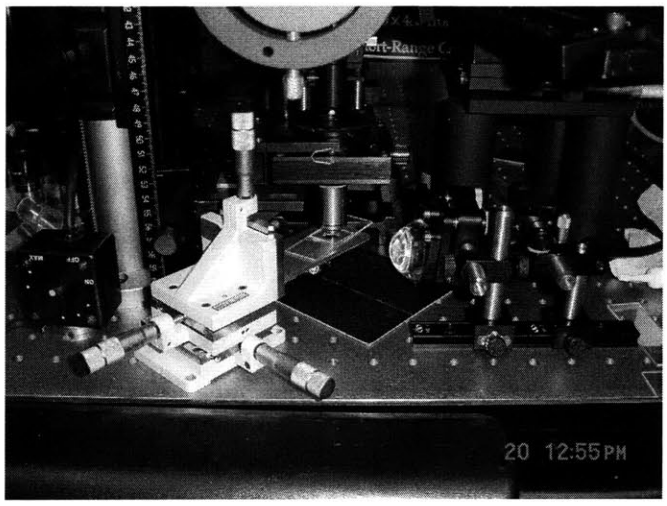


Fig. 3.3: Stage Setup

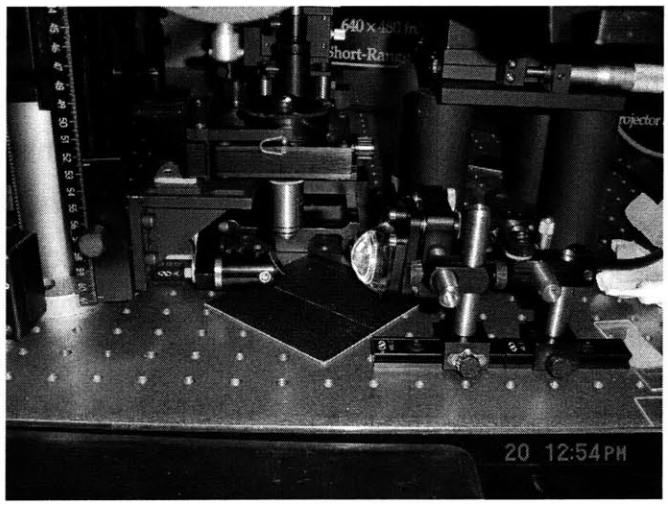


Fig. 3.4: Objective and Lighting Setup

light sources needed to be boosted. Instead of providing light from above the stage, the system provided light from below, giving the camera a bright field in which to work in. Most stan-

dard light sources also lacked the sheer intensity, and a large focusing lens had to be employed to maximize the amount of light at the stage level. (A slide with a sheet of paper was employed to roughly determine the focus at the stage.)

The power of the laser requires that the entire system be shielded in certain areas to prevent possible hazards. Since the DMD does diffract light, areas around the DMD had to be shrouded. Behind the dichroic mirror, a laser stop was placed. (The dichroic mirror did not have perfect reflectivity in the desired wavelength range, particularly because of the angle of incidence.)

To gain greater control over the location of bead trapping, a focusing lens is added to change the laser focus point. This allows for the camera to properly focus on the beads when trapped.

A beam expander was also included in the design to illuminate as many mirrors as possible, but was removed in the final system. Initially, a 20x beam expander was used fill the entire DMD array. This comes at a great cost in beam intensity, though. At worst, the beam expander throws away half of the overall intensity. Calculations were made on the amount of power delivered to the trap. The DMD itself has a 90% fill factor, 88% aluminum reflectivity, and 85% diffraction efficiency.

Added to the loss of roughly half of the power from the beam expander and transmission losses from uncoated lenses, only about 20% of the raw power from the laser reaches the trap.

From literature, the amount of force generated per unit power is approximately 0.1 pN/mW. [3] Given the amount of power from the laser, the maximum force would be approximately 1.0 pN. If further divided into multiple traps defined by the mirrors, there would be insufficient power in the trap. This forced the decision to reduce the actively used regions of the DMD to the raw laser beam diameter. Even with this reduced area, more than 1000 mirrors will be illuminated; a sufficient number to differentiate the separate traps.

The choice of laser was arbitrary, but if this were a system for actual use as a biological cell sorting assay, the light source would need to be in the infrared range to minimized the damage done to the cell. Research shows that cells absorb significantly less light at the longer wavelengths, and given the amount of light used, it is critical to minimize this level. It has been found that cells can literally explode from the laser illumination, an event coined as "opticution".[1] Using the infrared makes it difficult to do alignment, a problem that exists even with visible light.

The system requires a fairly strict alignment to obtain the best performance. The axis of the microscope objective must first be perpendicular to the coverslip to allow the best focusing and eliminate sources of stiction. The laser must also be aligned to fill the center of the objective. The laser below the dichroic mirror should be absolutely parallel to the optical axis of the objective. If it is not, the trap strength will be slightly reduced due to the angular displacement of the trap and the spherical aberration of the objective. Between the DMD and the dichroic mirror, the laser needs to follow a predetermined track at a set height. This allows for the trap focusing lens to be easily adjusted without major alignment corrections. As a result, almost every optical element in the system needed at least 3 axes of movement. The laser itself needed both angular and linear elements. The

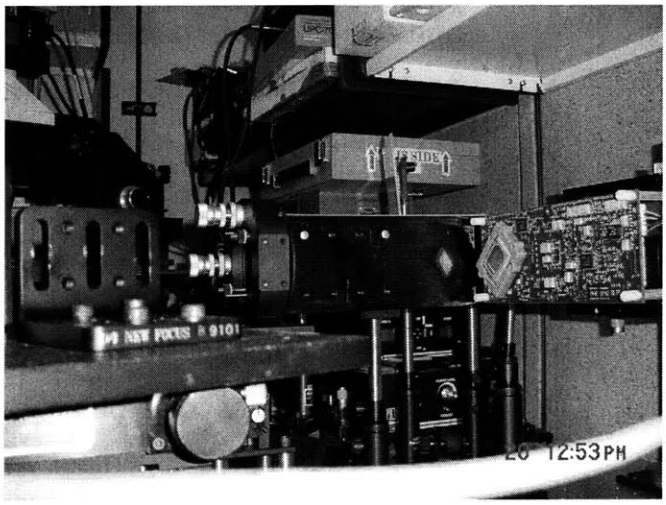


Fig. 3.5: Side View of System

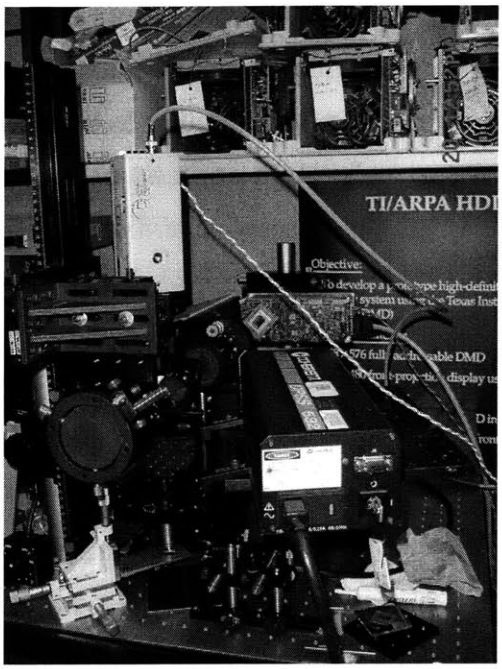


Fig. 3.6: Side View of System

DMD mount has one vertical, two angular (rotation and tilt), and one horizontal pieces. The focusing lens has vertical, horizontal, and angular adjustments to keep the laser in the center of the lens. The dichroic mirror needs two angular adjustments and a vertical one for centering. The microscope objective has two axial, two lateral, and one vertical components. One useful tool for alignment was to build a third structure with a target set at a specific height. By moving this test structure around the system, the laser could be aligned to be parallel to the optical table, reducing the alignment variability.

To connect the system to the computer and DMD, we added a color camera attached to a framegrabber and machine vision code. (Matrox Millenium 2 framegrabber and Matrox Imaging Library machine vision code) The machine vision algorithm is simply blob recognition. The code grabs a frame and simultaneously processes the previous frame. On the previous frame, the image is broken down into its component colors of blue, green, and red. The red image frame is binarized to an arbitrary user-defined threshold, and blob-finding algorithms run. For each blob, the system finds the maximum and minimum x/y locations and the blob centroid. These values are compared to previous values stored into a table. This correlates the blobs from one frame to the next. (The code only tracks blob that have moved less than its radius, i.e., the centroid of the current image is within the minimum bounding box.) The table also records the user-input of which blobs to track and where to move the desired blobs. From this user information, a new image to display on the DMD is generated.

The software also processes the green color frame for beam information. The green laser passes mostly through the system in a polarized state which the polarized filter removes before it reaches the camera. As the laser enters the liquid sample, it reflects and scatters slightly off the coverglass and water interface, giving an accurate estimate of the beam location, assum-

ing that the beam is travelling parallel to the objective optical axis. (This is another method to align the system as the sample is displaced vertically. By turning off most of the mirrors except those in the center of the DMD, the beam is narrowed. If vertical displacement of the sample causes lateral movement of the reflection, a misalignment is present and can be immediately corrected. This, incidentally, is the most accurate measurement of alignment since seeing the actual light profile of the trap makes it possible to see the real effects of changes in the optical system. This sanity check confirms that a pattern on the DMD can be transposed to a light intensity profile in the trap.) More importantly, when a bead enters the laser trap, the scattering off the bead causes an intense flash of green light. This strongly indicates a successful trapping and can be used to assist the tracking system.

## References

1. S. Smith et al., Am. J. Phys. 67, 26 (1999).
2. G. Wuite, Master's Thesis, 1996.
3. N. Simpson, Allen, L., Padgett, M., J. Modern Optics 43, 2485 (1996).

CHAPTER 4

# Optical Tweezer Performance

With the given system, we are able to successfully trap polystyrene spheres ranging in size from 1$\mu$m to 3$\mu$m. Three micron spheres are the easiest to track and therefore used for most measurements. The smaller spheres are stably trapped, but due to the initial transient motion of trapping, beads are pulled to far upwards and become stuck to the glass coverslip. Spheres smaller than 1$\mu$m are also tested, but the bead concentration is too high to pick out individual spheres and high fluid flow rates made spheres jump into and immediately out of the trap. One noticeable phenomenon noticed was these small beads entering the trap, changing brightness as the beads rose towards the beam focus, and exiting on the opposite side.

Estimates of the axial trap strength are made inserting the effects of gravity into the force equation. Assuming that the effective mass is equal to the real mass times the ratio of the density of the beads and water, we calculated the amount of force required to keep the beads suspended. For the 3$\mu$m bead, approximately 0.007pN are required. This measurement has a high degree of error though. The density of the beads and water are difficult to estimate. The polystyrene can vary in density from 1.04 to 1.06, and since tap water was used, its specific gravity is likely greater than 1. The beads themselves also vary in size, with a nominal size of 2.837$\mu$m and a standard deviation of 0.133$\mu$m. This estimate of trap strength is also a lower boundary on the actual trap strength, since we did not push the limits of the trap.

The DMD, though, allows for spatially shuttering the light. Reducing the beam to a 3 mirror/pixel radius still had successful trapping, but just barely. Any less and the bead escapes. Assuming the laser has relatively equal power across the radius, this equates to approximately 0.96mW of power delivered into the trap and an efficiency factor of 0.0016. This is much lower than standard optical traps but should be expected given the narrow cone of light used. Instead of using the entire optical area of the microscope objective, only a small sliver is

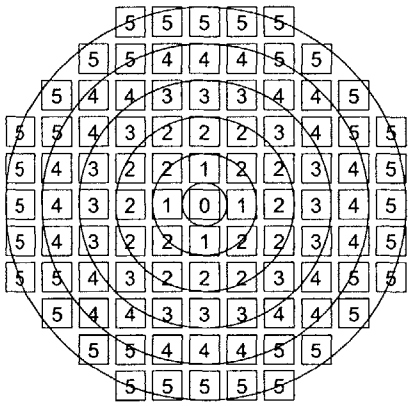

Fig. 4.1: Radius/Pixel Illumination

illuminated. The illumination cone of the trap is very narrow with few oblique rays. The end result is a very inefficient trap.

Since the DMD can shutter the light in more forms than a simple pinhole, we modified the pattern to be a donut. An equivalent trap was generated by changing the profile from a solid circle with 3 pixel diameter to a donut with outer diameter of 3 pixels and an inner diameter of 2 pixels. This increases the effective Q to 0.0029. This is still a very inefficient trap, but shows that the DMD could make a trap much more efficient. This donut profile also seemed to have a greater incidence of stiction to the cover slip. This suggests that the gradient forces overbalanced the scattering force and made the stable trapping point a bit further upstream than with the pinhole profile.

Lateral measurements were also made. In this case, no provisions were made to specifically test lateral trap strength, but in the course of experimenting, a capillary effect occurred within the sample. As the experiment ran, liquid evaporating from the edge drew liquid from the center, carrying the beads with it. Initially this was a problem as the sample dried up within 15 minutes. With the video recording capabilities of the system, though, I was able to examine the tape and find examples of stable trapping with the lateral flow. Once a bead was successfully trapped, a bead floating in the liquid is measured frame by frame, giving an estimate of the liquid velocity. Assuming laminar flow, we estimate the lateral strength as 0.45pN. To ensure that the bead was trapped and not stuck to the coverslip, any subject bead must escape the trap at a later point. This leads to an accurate measurement of the maximum trap strength assuming that the velocity can be accurately determined and conditions are still in a laminar flow phase.

Integrating the vision system also showed promising results. The camera/framegrabber/software processing/binary formatter combination had no significant problems. The vision system was able to discriminate between the imaged beads and process each frame at video frame rates. The binary formatter and PCI interface were also able to absorb the high data burst rates required to maintain the high refresh rate. The binary formatter,

while designed to exclusively control the PCI, was able to successful share the bus with a frame grabber, a high data rate device.

When combined fully with the laser and optics system, though, the feedback system completely failed. Although the computer attempted to direct the spheres by changing the DMD pattern, I was not able to demonstrate a stable trapping scheme that would directly correlate to distinct trapping locations as viewed by the CCD camera. On closer inspection, the fault lies with the interaction of the light with the particle. While simulations showed that the bead could be stably trapped at a point further downstream, the actual testing did not show any evidence of the lower stable trapping point. Attempts were made to move the bead at the point closer to the beam focus. These were marginally successful since some bead movement was detected. The movement, though, had a maximum displacement of 1 um before the bead suffered from stiction to the coverslip. In addition, the bead could only be moved inwards towards the vertical optical axis. A bead could be trapped with an angled beam and drawn towards the center, but any attempt to reverse this movement resulted in instant stiction to the coverslip.

The lack of the lower trap position, though, effectively dooms the entire sorting assay. Looking closer at the theory, there are indications that the theory as applied is not correct. While the ray-optic theory works for focused light with a Gaussian distribution, altering the intensity distribution may mean that the model will not be entirely correct. When looking at the Rayleigh regime model of gradient and scattering forces, the trap can only be stable where there is a significant intensity gradient. If a trap were to be formed well below the focus, the axial gradient would be minimal at best. Clearly, a system to use the DMD for a cell sorting assay could not use this method.

One way of making this assay work properly would require changing the optical system dramatically. Instead of having all of the light coming to a single focus, each mirror would have to direct a ray of light to a separate focus point. These focus points would lie on a single plane, thus keeping the beads in focus and under control. By turning on or off each mirror, an intensity gradient could be created in the lateral direction. An axial intensity gradient is created by each beam coming to the separate focus. Ideally, a beam formed by a single mirror would have to fill the entire objective back while entering the objective at a distinct angle. Filling the entire back opening of the objective causes a steep axial gradient as the rays come to a diffraction-limited point. The distinct entry angle means that

these diffraction-limited focal points will be at distinct locations. As long as each beam is identical in terms of parallelism, the focus points will be along the same plane. Making this optical system, though, is well beyond my current abilities with optics.

Another failing of the system was the common occurrence of stiction of beads that were under control by the trap. This was caused by the low focus point of the microscope objective. With the given objective, it was impossible to properly image beads more than a few tens of microns into the sample.

In conclusion, I have shown that the DMD can be used to spatially modulate monochromatic light intensity. When used in conjunction with the binary formatter, the DMD provides real-time, adjustable spatial shuttering for a variety of applications. In this particular application of optical tweezers, the applied mode of operation was unsuccessful at creating a cell sorting assay, but provides useful insights about the operation of optical tweezers.

CHAPTER A

# *Ray-Optic Simulation*

## Angle of Incidence

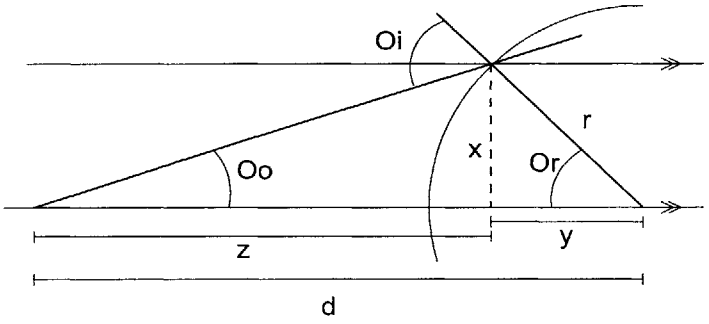


$$\theta_i = \theta_r + \theta_o$$

$$\sin\theta_r = \frac{x}{r},\ \tan\theta_o = \frac{x}{z}$$

$$\cos\theta_r = \frac{y}{r} \Rightarrow y = r\cos\theta_r$$

$$z = d - y$$

$$r\sin\theta_r = z\tan\theta_o \Rightarrow \tan\theta_o = \frac{r\sin\theta_r}{d - r\cos\theta_r}$$

$$\theta_o = \operatorname{atan}\frac{r\sin\theta_r}{d - r\cos\theta_r} \qquad ,0 \le \theta_r \le \operatorname{acos}\frac{r}{d}$$

$$0 \le \theta_o \le \frac{\pi}{2} - \operatorname{acos}\frac{r}{d}$$

## Refraction and Reflection Angles

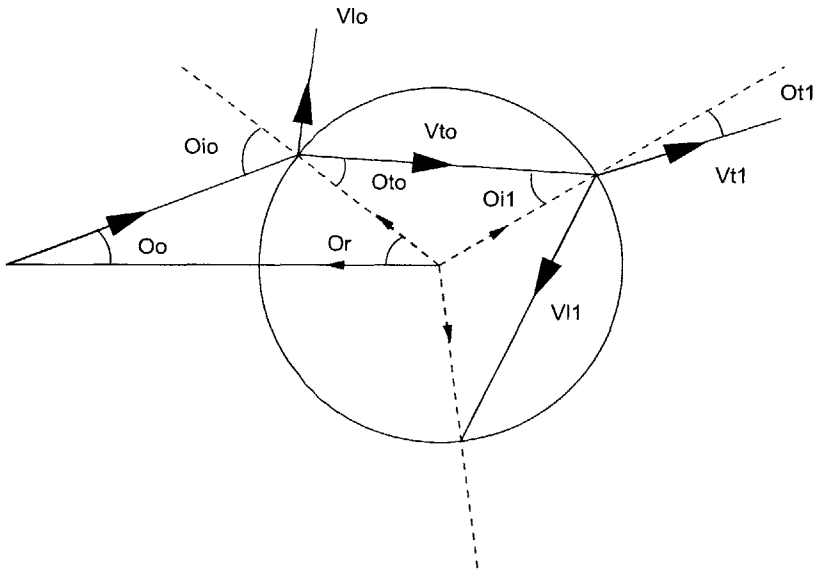


### Angles at 1st interface

$$\theta_r = \angle\vec{V}_{r0}$$

$$\theta_{i0} = \theta_o + \theta_r$$

$$\angle\vec{V}_{l0} = \angle\vec{V}_{r0} + \theta_{i0}$$

$$\angle\hat{V}_{t0} = \angle\hat{V}_{r0} + (\pi - \theta_{t0})$$

$\theta_{t0} = f_{12}(\theta_{i0})$ Snell's Law of Refraction

**Angles at 2nd interface**

$$\theta_{i1} = \theta_{t0}$$

$$\angle\hat{V}_{r1} = \angle\hat{V}_{r0} + (\pi - 2\theta_{t0})$$

$$\angle\hat{V}_{l1} = \angle\hat{V}_{r1} + (\pi - \theta_{i1}) = \angle\hat{V}_{r1} + (\pi - \theta_{t0})$$

$$\angle\hat{V}_{t1} = \angle\hat{V}_{r1} + \theta_{t1}$$

$$\theta_{t1} = f_{21}(\theta_{i1}) = f_{21}(\theta_{t0}) = f_{21}(f_{12}(\theta_{i0}))$$

**Angles at 3rd interface**

$$\theta_{i2} = \theta_{t1} = \theta_{i1} = \theta_{t0}$$

$$\angle\hat{V}_{r2} = \angle\hat{V}_{r1} + (\pi - 2\theta_{t0})$$

$$\angle\hat{V}_{l1} = \angle\hat{V}_{r2} + (\pi - \theta_{t0})$$

$$\angle\hat{V}_{t1} = \angle\hat{V}_{r2} + \theta_{t2} = \angle\hat{V}_{r0} + \theta_{t1}$$

**Snell's Law**

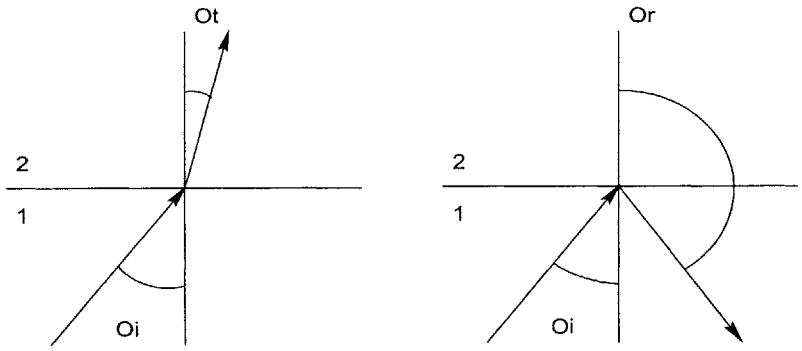

$$\frac{\sin\theta_i}{\sin\theta_t} = \frac{n_1}{n_2}$$

$$\theta_i = \pi - \theta_r$$

CHAPTER B

# Ray-Optic Model Simulation Code

```
// rayoptic.cpp : Defines the entry point for the console application.
//

#include "stdafx.h"
#include <math.h>

#define WATER 1.33
#define GLASS 1.55
#define ERROR 0.001
#define PI 3.141592653589793238462
 //3.14159265358979323846264338327950

struct VECTOR
{
double amplitude;
double angle;
};

//
//
//
double FindThetaR(double ThetaO, double Radius, double X, double Y,
  double HighThetaR, double LowThetaR, int iterations)
```

```
{
double dThetaO;
double avgThetaR=(HighThetaR+LowThetaR)/2;
dThetaO=atan((Radius*sin(avgThetaR)+Y)/(X+Radius*cos(avgThetaR)));
if ((dThetaO<=(ThetaO+ERROR)) && (dThetaO>=(ThetaO-ERROR)))
{
return avgThetaR;
}
else if ((iterations<=0) || (HighThetaR==LowThetaR))
{
return 999; //error--no solution
}
else
{
if (dThetaO<ThetaO)
return FindThetaR(ThetaO,Radius,X,Y,HighThetaR,avgThetaR,iterations--);
else
return FindThetaR(ThetaO,Radius,X,Y,avgThetaR,LowThetaR,iterations--);
}
};

double diag(double x,double y)
{
return sqrt(x*x+y*y);
};

VECTOR AddVectors(VECTOR V1, VECTOR V2)
{
VECTOR result;
double vx=V1.amplitude*cos(V1.angle)+V2.amplitude*cos(V2.angle);
double vy=V1.amplitude*sin(V1.angle)+V2.amplitude*sin(V2.angle);
result.amplitude=diag(vx,vy);
result.angle=(vx==0?0:atan2(vy,vx));
return result;
};

VECTOR DiffVector(VECTOR incident, VECTOR reflected)
{
VECTOR result;
double vx=incident.amplitude*cos(incident.angle)-reflected.ampli-
tude*cos(reflected.angle);
```

```
double vy=incident.amplitude*sin(incident.angle)-reflected.ampli-
tude*sin(reflected.angle);
result.amplitude=diag(vx,vy);
result.angle=(vx==0?0:atan2(vy,vx));
return result;
};

//
//
//ignore polarization for now--assume all rays are // to incident plane
//laser is linearly polarized to start.
VECTOR ForceFromRayParallel(VECTOR incident,double ThetaR)
{
double Theta10=ThetaR+incident.angle;
double ThetaT0=asin(WATER/GLASS*sin(Theta10));

double Tparall0=2*WATER*cos(Theta10)/
(GLASS*cos(Theta10)+WATER*cos(ThetaT0))*incident.amplitude;
double Rparall0=(GLASS*cos(Theta10)-WATER*cos(ThetaT0))/
(GLASS*cos(Theta10)+WATER*cos(ThetaT0))*incident.amplitude;

VECTOR Vlo={Rparall0,ThetaR+Theta10};

double ThetaT1=asin(GLASS/WATER*sin(ThetaT0));
double cTparall=2*GLASS*cos(ThetaT0)/
(WATER*cos(ThetaT0)+GLASS*cos(ThetaT1));
double cRparall=(WATER*cos(ThetaT0)-GLASS*cos(ThetaT1))/
(WATER*cos(ThetaT0)+GLASS*cos(ThetaT1));

VECTOR Vt1={Tparall0*pow(cRparall,0)*cTparall,ThetaT1+ThetaR+1*(PI-
2*ThetaT0)};
VECTOR Vt2={Tparall0*pow(cRparall,1)*cTparall,ThetaT1+ThetaR+2*(PI-
2*ThetaT0)};
VECTOR Vt3={Tparall0*pow(cRparall,2)*cTparall,ThetaT1+ThetaR+3*(PI-
2*ThetaT0)};
VECTOR Vt4={Tparall0*pow(cRparall,3)*cTparall,ThetaT1+ThetaR+4*(PI-
2*ThetaT0)};

VECTOR VTotal=AddVectors(Vlo,Vt1);
VTotal=AddVectors(VTotal,Vt2);
VTotal=AddVectors(VTotal,Vt3);
VTotal=AddVectors(VTotal,Vt4);
```

```
incident.angle=PI-incident.angle;
VECTOR VForce=DiffVector(incident,VTotal);
return VForce;
};

VECTOR ForceFromRayPerpindicular(VECTOR incident,double ThetaR)
{
double ThetaI0=ThetaR+incident.angle;
double ThetaT0=asin(WATER/GLASS*sin(ThetaI0));

double Tperpin0=2*WATER*cos(ThetaI0)/
(WATER*cos(ThetaI0)+GLASS*cos(ThetaT0))*incident.amplitude;
double Rperpin0=(WATER*cos(ThetaI0)-GLASS*cos(ThetaT0))/
(WATER*cos(ThetaI0)+GLASS*cos(ThetaT0))*incident.amplitude;
VECTOR Vlo={Rperpin0,ThetaR+ThetaI0};

double ThetaT1=asin(GLASS/WATER*sin(ThetaT0));
double cTperpin=2*GLASS*cos(ThetaT0)/
(GLASS*cos(ThetaT0)+WATER*cos(ThetaT1));
double cRperpin=(GLASS*cos(ThetaT0)-WATER*cos(ThetaT1))/
(GLASS*cos(ThetaT0)+WATER*cos(ThetaT1));

VECTOR Vt1={Tperpin0*pow(cRperpin,0)*cTperpin,ThetaT1+ThetaR+1*(PI-
2*ThetaT0)};
VECTOR Vt2={Tperpin0*pow(cRperpin,1)*cTperpin,ThetaT1+ThetaR+2*(PI-
2*ThetaT0)};
VECTOR Vt3={Tperpin0*pow(cRperpin,2)*cTperpin,ThetaT1+ThetaR+3*(PI-
2*ThetaT0)};
VECTOR Vt4={Tperpin0*pow(cRperpin,3)*cTperpin,ThetaT1+ThetaR+4*(PI-
2*ThetaT0)};
/*printf("%f, %f\n%f, %f\n%f, %f\n%f %f\n",Vlo.amplitude,Vlo.angle,
Vt1.amplitude,Vt1.angle,Vt2.amplitude,Vt2.angle,Vt3.amplitude,Vt3.angle,
Vt4.amplitude,Vt4.angle);*/

VECTOR VTotal=AddVectors(Vlo,Vt1);
VTotal=AddVectors(VTotal,Vt2);
VTotal=AddVectors(VTotal,Vt3);
VTotal=AddVectors(VTotal,Vt4);
VECTOR VForce=DiffVector(incident,VTotal);
return VForce;
};
```

```
VECTOR ForceOnSphere(double X, double Y, double Radius)
{
VECTOR V[5];
VECTOR Result[5];
VECTOR Sum={0,0};
double high=acos(Radius/X);
double low=-high;
V[0].amplitude=1;
V[1].amplitude=0;
V[2].amplitude=58;
V[3].amplitude=0;
V[4].amplitude=1;

V[0].angle=PI/50;
V[1].angle=PI/75;
V[2].angle=0;
V[3].angle=-PI/75;
V[4].angle=-PI/50;

for (int i=0;i<5;i++)
{
Result[i]=ForceFromRayParallel(V[i],Find-
ThetaR(V[i].angle,Radius,X,Y,high,low,10));
//printf("%f,%f \n",Result[i].amplitude,Result[i].angle);
Sum=AddVectors(Sum,Result[i]);
}
return Sum;
//result indicates light vector--reverse is force vector
};

//need to write data to file
//define light source(angle/intensity)
//define new bead location(given force, move
//given light source, initial bead location, track bead movement until movement is
neglible.

//

void main()
{
double r=3;
```

```
double x=10;
double y=0;
VECTOR a;
for (int i=-1;i<2;i++)
{
a=ForceOnSphere(x,y+i*0.1,r);
printf("result: %d: %f,%f\n",i, a.amplitude,a.angle);
}
getchar();

}
```

CHAPTER C

# Framegrabber to DMD Feedback Code

```
// OTfeedback.cpp : Defines the entry point for the console application.
//

#include "stdafx.h"
#include <mil.h>
#include <windows.h>
#include <conio.h>

/* Minimum and maximum area of blobs. */
#define MIN_BLOB_AREA 50L
#define MAX_BLOB_AREA 50000L

/* Radius of the smallest particles to keep. */
#define MIN_BLOB_RADIUS      3L
```

```
/* Size and color of the cross used to mark centers of gravity. */
#define CROSS_SIZE10L
#define VECTOR_SIZE10L
#define BLACK250L
#define WHITE0L

/* Utility functions prototype */
void DrawCross(MIL_ID ImageId, double CenterX, double CenterY, bool Bold);
void DrawVector(MIL_ID ImageId, double CenterX, double CenterY, int ShiftX, int
ShiftY);

void main(void)
{
  MIL_ID MilApplication,/* Application identifier.*/
       MilSystem,/* System identifier.*/
       MilDisplay,/* Display identifier.*/
 MilDigitizer,/* Digitizer identifier.*/
 MilColorImage[2],/* Color Image identifier.*/
 MilGrayImage[2],/* Grayscale Image identifier.*/
 MilBinImage[2],/* Binary Image identifier.*/
 MilOutImage[2],/* Binary Image identifier.*/
       BlobResult,        /* Blob result buffer identifier. */
       FeatureList;       /* Feature list identifier.*/
const int SizeX=512, SizeY=384;
const int cX=0,cY=1,cM=2,tX=3,tY=4;
const int MAX_BLOBS=50;

int cframe=0,nframe=1;
```

```
long i,j,n;

int Threshold=100;
long TotalBlobs,/* Total number of blobs.        */
     CogX[MAX_BLOBS],/* X coordinate of center of gravity. */
     CogY[MAX_BLOBS],/* Y coordinate of center of gravity. */
CogXmin[MAX_BLOBS],/* Minimum X value*/
CogXmax[MAX_BLOBS],/* Maximum X value*/
CogYmin[MAX_BLOBS],/* Minimum Y value*/
CogYmax[MAX_BLOBS],/* Maximum Y value*/
CogXfer[MAX_BLOBS],/* X Feret*/
CogYfer[MAX_BLOBS]; /* Y Feret*/
int select[MAX_BLOBS][5];
int sel=0;
int shiftX,shiftY;
char Output[384][64];
int ch;
bool go=true;

  /* Allocate defaults */
P9050_HANDLE hPlx = NULL;
if (P9050_Open(&hPlx,0x10b5,0x9050,0,0)) //opens BF card
{
//DWORD dwStatus = BF_Status(hPlx);
// TODO: Add a check for 0xfff... as a PCI bus error on init.
//POWERON
P9050_FlagDMD(hPlx, REG_COMMAND14, BIT_POWER_UP,
REG_CMD_WRITE, true);  //power on
```

```
P9050_FlagDMD(hPlx, REG_COMMAND10, BIT_BOARD_RESET,
REG_CMD_WRITE, true); //board reset

P9050_FlagDMD(hPlx, REG_COMMAND10, BIT_BOARD_RESET,
REG_CMD_WRITE, false);

P9050_WriteRegister(hPlx, REG_PATTERN_START_ADDRESS, 0x0); //sets
pattern address


//Allocate MIL resources

MappAllocDefault(M_SETUP, &MilApplication, &MilSystem, &MilDisplay,
M_NULL, M_NULL);

//Digitizer

MdigAlloc(MilSystem,M_DEFAULT,"NTSC",M_DEFAULT,&MilDigitizer); //initial-
izes digitizer

MdigControl(MilDigitizer,M_GRAB_SCALE, 0.8); //grab of 0.8 of 640x480

MdigControl(MilDigitizer,M_GRAB_MODE,M_ASYNCHRONOUS); //asynchro-
nous mode--grab and continue

//Image buffers

for (i=0;i<2;i++) { //allocate processing buffers

MbufAllocColor(MilSys-
tem,3,SizeX,SizeY,8+M_UNSIGNED,M_GRAB+M_IMAGE,&MilColorImage[i]);

MbufAlloc2d(MilSys-
tem,SizeX,SizeY,8+M_UNSIGNED,M_PROC+M_IMAGE,&MilGrayImage[i]);

MbufAlloc2d(MilSys-
tem,SizeX,SizeY,1+M_UNSIGNED,M_PROC+M_DISP+M_IMAGE,&MilBinIm-
age[i]);

MbufAlloc2d(MilSys-
tem,SizeX,SizeY,1+M_UNSIGNED,M_PROC+M_IMAGE,&MilOutImage[i]);

}

//Blob analysis buffers

MblobAllocResult(MilSystem,&BlobResult);

MblobControl(BlobResult,M_IDENTIFIER_TYPE,M_BINARY);

MblobAllocFeatureList(MilSystem,&FeatureList);
```

```
MblobSelectFeature(FeatureList,M_CENTER_OF_GRAVITY);
MblobSelectFeature(FeatureList,M_BOX);
//clear table of blob position, move, destination
for (i=0;i<MAX_BLOBS;i++) { select[i][cX]=0; }
//grab and process loop
if (getchar()=='a') go=false;
while (go)
{
cframe=nframe;
nframe=1-cframe; //swap display and processing frames
MdispSelect(MilDisplay,MilBinImage[nframe]); //show old binary frame
//MdispSelect(MilOutImage[nframe]);
MdigGrab(MilDigitizer,MilColorImage[nframe]); //grab next frame
MbufCopyColor(MilColorImage[cframe],MilGrayImage[cframe],M_RED); //pull red
color (no green!)
MimBinarize(MilGrayImage[cframe],MilBinIm-
age[cframe],M_GREATER_OR_EQUAL,Threshold, M_NULL); //binarize
MimOpen(MilBinImage[cframe], MilBinImage[cframe], MIN_BLOB_RADIUS,
M_BINARY); //OPEN (make blobs larger)
MblobCalculate(MilBinImage[cframe], M_NULL, FeatureList, BlobResult); //find
blobs
MblobSelect(BlobResult, M_EXCLUDE, M_AREA, M_LESS_OR_EQUAL,
MIN_BLOB_AREA, M_NULL);  //exclude small blobs
MblobGetNumber(BlobResult, &TotalBlobs);  //get number of blobs
if(TotalBlobs < MAX_BLOBS) { //get parameters of blobs
MblobGetResult(BlobResult, M_CENTER_OF_GRAVITY_X+M_TYPE_LONG,
CogX);
MblobGetResult(BlobResult, M_CENTER_OF_GRAVITY_Y+M_TYPE_LONG,
CogY);
MblobGetResult(BlobResult, M_BOX_X_MIN+M_TYPE_LONG, CogXmin);
```

```
MblobGetResult(BlobResult, M_BOX_X_MAX+M_TYPE_LONG, CogXmax);
MblobGetResult(BlobResult, M_BOX_Y_MIN+M_TYPE_LONG, CogYmin);
MblobGetResult(BlobResult, M_BOX_Y_MAX+M_TYPE_LONG, CogYmax);
MblobGetResult(BlobResult, M_FERET_X+M_TYPE_LONG, CogXfer);
MblobGetResult(BlobResult, M_FERET_Y+M_TYPE_LONG, CogYfer);
}
MbufClear(MilOutImage[cframe],0); //clear output buffer
for (i=0;i<MAX_BLOBS;i++) { //match actual blobs with coordinates in table
if (select[i][cX]!=0) {
for (j=0;j<TotalBlobs;j++)
{
if ((select[i][cX]>CogXmin[j]) && (select[i][cX]<CogXmax[j]) &&
(select[i][cY]>CogYmin[j]) && (select[i][cY]<CogYmax[j])) {
if (i==0) { sel=j; }
select[i][cX]=CogX[j];
select[i][cY]=CogY[j];
//calculate move to
switch (select[i][cM])
{
case 1: shiftX= 1; shiftY=-1; break; //down, left
case 2: shiftX= 1; shiftY= 0; break; //down
case 3: shiftX= 1; shiftY= 1; break; //down, right
case 4: shiftX= 0; shiftY=-1; break; //left
case 5: shiftX= 0; shiftY= 0; break; //hold
case 6: shiftX= 0; shiftY= 1; break; //right
case 7: shiftX=-1; shiftY=-1; break; //up, left;
case 8: shiftX=-1; shiftY= 0; break; //up
case 9: shiftX=-1; shiftY= 1; break; //up, right;
```

```
}
DrawVector(MilBinImage[cframe],CogX[j],CogY[j], shiftX, shiftY);
MbufCopyColor2d(MilBinImage[cframe],MilOutImage[cframe],
0,CogXmin[j],CogYmin[j],
0,(CogXmin[j]+shiftX),(CogYmin[j]+shiftY),
CogXfer[j],CogYfer[j]); //copy & shift blob
}
}
}
}
for (i=0;i<TotalBlobs; i++){ //box blobs
MgraRect(M_DEFAULT,MilBinImage[cframe], CogXmin[i],CogYmin[i], CogX-
max[i],CogYmax[i]);
}
DrawCross(MilBinImage[cframe], CogX[sel],CogY[sel], select[0][cX]?true:false);
MbufGet(MilOutImage[cframe],&Output); //send buffer to array
//board reset??
P9050_FlagDMD(hPlx, REG_COMMAND10, BIT_BOARD_RESET,
REG_CMD_WRITE, true);
P9050_FlagDMD(hPlx, REG_COMMAND10, BIT_BOARD_RESET,
REG_CMD_WRITE, false);
//for (i=0;i<64;i++) printf("%2x ",Output[0][i]);
char cMask;DWORD add,lData,hData, addr=0x0; int iRow,iBit,iByte;
for (iRow=0;iRow<384;iRow++) { //T-B //for (iRow=383;iRow>=0;iRow--) { //B-T
for (i=0;i<2;i++) {
for (iBit=7;iBit>=0;iBit--) { //for (iBit=0;iBit<8;iBit++) { //R-L
lData=0; hData=0; cMask=0x80>>iBit;
for (iByte=0;iByte<32;iByte++) {
add=0x80000000>>iByte;
```

```
if (Output[iRow][31-iByte] & cMask) lData+=add;
if (Output[iRow][63-iByte] & cMask) hData+=add;
}
P9050_WriteMemory(hPlx,addr,lData);addr+=0x4;
for (n=0;n<40;n++) {}
P9050_WriteMemory(hPlx,addr,hData);addr+=0x4;
for (n=0;n<40;n++) {}
P9050_WriteMemory(hPlx,addr,lData);addr+=0x4;
for (n=0;n<40;n++) {}
P9050_WriteMemory(hPlx,addr,hData);addr+=0x4;
}
}
if (iRow%8==7) {
P9050_FlagDMD(hPlx, REG_COMMAND10, BIT_WRITE, true, true);
int iCountdown = 1024; bool fFlag;
do { fFlag = P9050_FlagDMD(hPlx, REG_STATUS, BIT_WRITE_FIFO_FULL,
false, false);
} while (fFlag && iCountdown--);
if (iCountdown < 0) {
iCountdown = -1;
printf("Countdown invoked");
}
}
}
P9050_FlagDMD(hPlx, REG_COMMAND10, BIT_DMD_LOAD, true, true); //load
pattern
P9050_FlagDMD(hPlx, REG_COMMAND10, BIT_DMD_RESET, true, true); //
dmd reset pulse
if (_kbhit()) {
```

```
ch=_getch();
if ((ch==0x0) || (ch==0xe0)) {
switch (_getch()) //ch=_getch();
{
case ';': break;
case '<': break;
case '=': break;
case '>': break;
case '?': sel+=1; if(sel>TotalBlobs) sel=0; break; //F5
case '@':
if (select[0][cX]) {
select[0][cX]=CogX[sel];
select[0][cY]=CogY[sel];
} else { select[0][cX]=0; } break; //F6
case 'A': break;
case 'B': break;
case 'C': break;
case 'D': go=false; break;
case 'H': if (select[0][cM]<7) select[0][cM]+=3; break; //up
case 'K': if ((select[0][cM]%3)!=1) select[0][cM]-=1; break; //left
case 'P': if (select[0][cM]>3) select[0][cM]-=3; break; //down
case 'M': if ((select[0][cM]%3)!=0) select[0][cM]+=1; break; //right
case 'R': break;
case 'G': Threshold+=8; break;
case 'I': break;
case 'S': Threshold+=1; break;
case 'O': Threshold-=8; break;
case 'Q': Threshold-=1; break;
```

```
}
}
}
//set next destination
} //end loop
printf("%d",Threshold);
//POWEROFF
//release resources
MblobFree(FeatureList);
MblobFree(BlobResult);
for (i=0;i<2;i++) {
MbufFree(MilColorImage[i]);
MbufFree(MilGrayImage[i]);
MbufFree(MilBinImage[i]);
MbufFree(MilOutImage[i]);
}
MdigFree(MilDigitizer);
MappFreeDefault(MilApplication,MilSystem,MilDisplay,M_NULL,M_NULL);
P9050_FlagDMD(hPlx, REG_COMMAND14, BIT_POWER_UP,
REG_CMD_WRITE, false); //power down
P9050_Close(hPlx);
  } else {
  printf("%s",P9050_ErrorString);
  getchar();
  }
}
```

```
/* Draw a cross at the specified position. */
void DrawCross(MIL_ID ImageId, double CenterX, double CenterY, bool Bold)
{
int Thick=0;
if (Bold) {Thick=2;}
MgraColor(M_DEFAULT,0);
MgraRectFill(M_DEFAULT, ImageId,
(long)(CenterX+.5)-(CROSS_SIZE/2), (long)(CenterY+.5-Thick),
(long)(CenterX+.5)+(CROSS_SIZE/2), (long)(CenterY+.5+Thick));
MgraLine(M_DEFAULT, ImageId,
(long)(CenterX+.5-Thick), (long)(CenterY+.5)-(CROSS_SIZE/2),
(long)(CenterX+.5+Thick), (long)(CenterY+.5)+(CROSS_SIZE/2));
}

void DrawVector(MIL_ID ImageId, double CenterX, double CenterY, int ShiftX, int
ShiftY)
{
MgraLine(M_DEFAULT, ImageId,
(long)(CenterX+.5), (long)(CenterY+.5),
(long)(CenterX+.5)+(ShiftX*VECTOR_SIZE),
(long)(CenterY+.5)+(ShiftY*VECTOR_SIZE));

}
```

CHAPTER D

# *Optical Tweezer Video Images*

These sets of images were taken from video of 3$\mu$m diameter polystyrene spheres immersed in tap water as they floated by the optical trap. The images proceed from left to right, top to bottom, and are spaced 1/30 second apart. The first 16 images show 2 beads, the center and brighter bead being successfully trapped. The green fringing around this bead is the scattering of the trapping laser light. The darker bead is carried by the flow of fluid from left to right. (The brightness of the bead indicates the axial position of the bead. A brighter bead is closer to the microscope objective lens.) Fluid velocity is estimated at 15$\mu$m/s.

The second set shows a third bead entering the picture from the left. The previous trapped bead has become dislodged from the trap and escapes (frame 8). At frame 13, a bright flash of green indicates that the third bead has become trapped. Also note the bead center has lightened considerably as the trap has drawn the bead upward as well as laterally.

The third set of images show the third bead trapped until a large clump of spheres collides with and carries the third bead away. This mass of beads is far too heavy and large for this particular beam configuration to capture. Other images have shown that up to 4 beads can be simultaneously trapped in a similar beam.

The final set demonstrates that manual movement of the beam via DMD mirror states does translate into changing the position of the beam and resultingly the bead position. The aiming point moves from the top left part of the screen to the center in half a second, dragging the bead along.

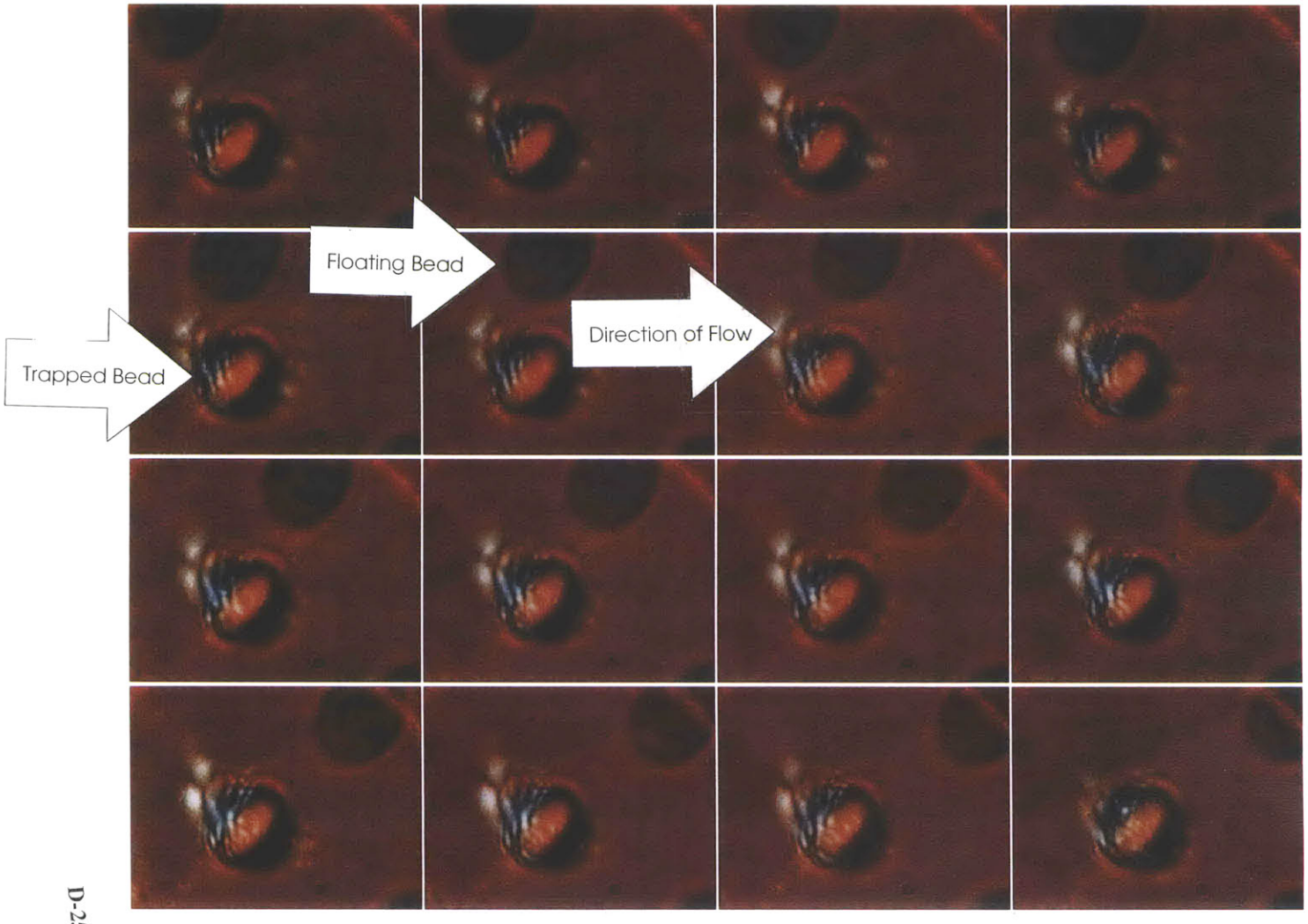


Figure D.1: Bead Captured With Velocity Measurement

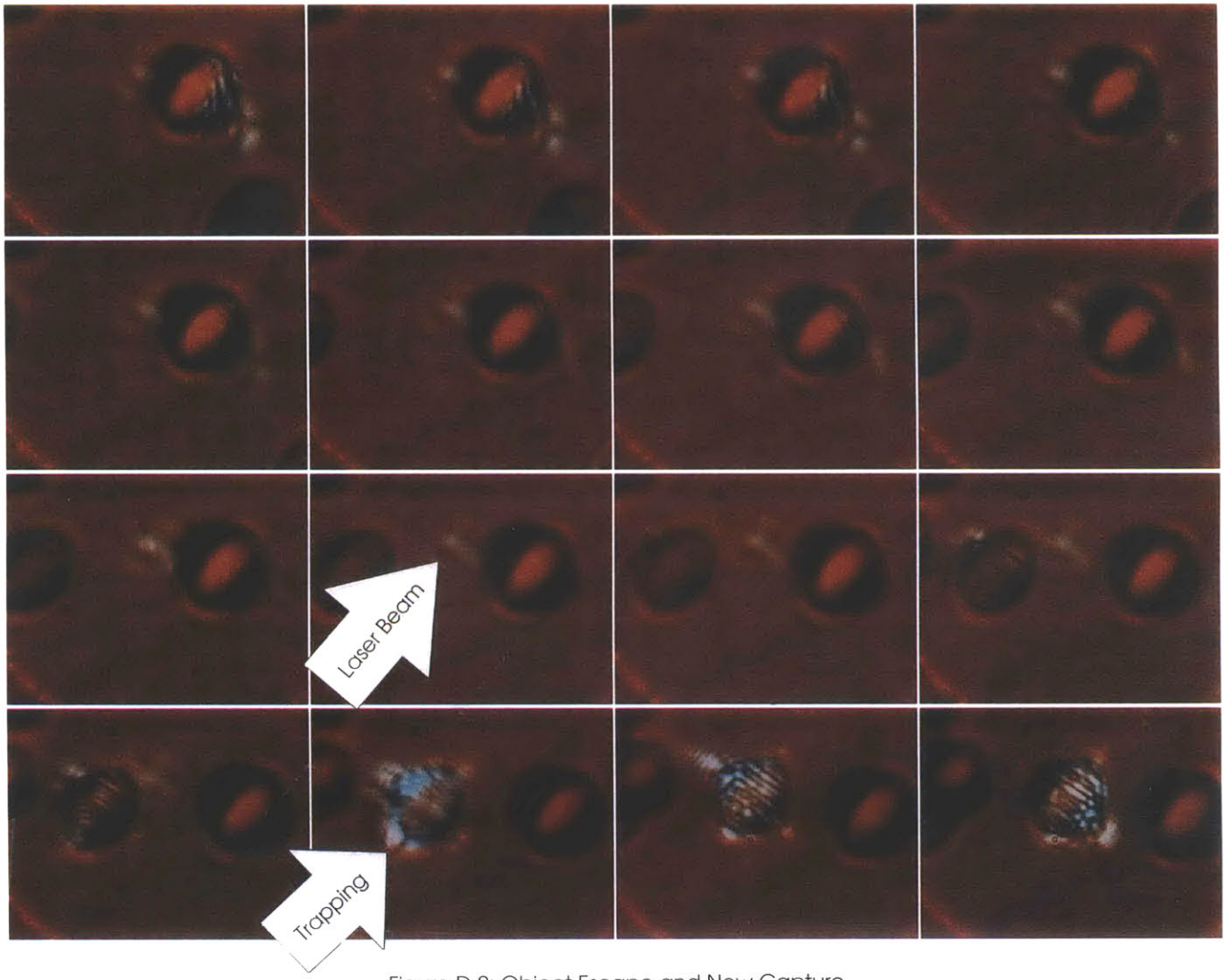


Figure D.2: Object Escape and New Capture

Figure D.3: Verification of Trapping

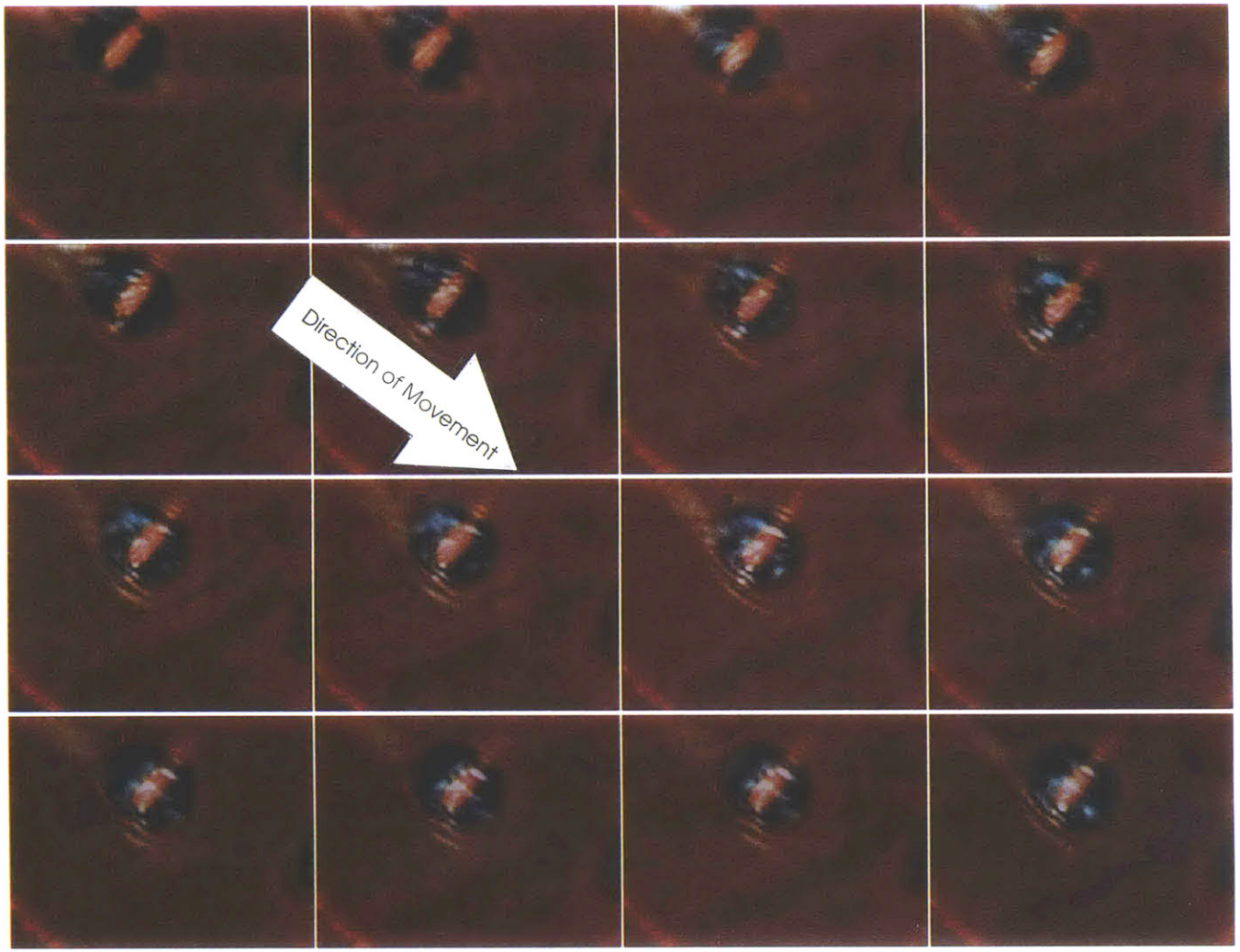


Figure D.4: Bead Movement by Altering DMD mirrors